

Received by BNL

## THE RATIONALE FOR RHIC IN THE CONTEXT OF RECENT A+A DATA

C. Chasman, O. Hansen, and H. E. Wegner  
Brookhaven National Laboratory, Upton, NY 11973 USA

BNL--41534

### 1. Introduction

DE88 015818

RHIC stands for Relativistic Heavy Ion Collider. RHIC is designed as a collider with two beams and four intersections. The beams may be different, each can have a mass number from 1 to  $\approx 200$  (in practice probably  $^{197}\text{Au}$ ). The  $\sqrt{s}$  for Au+Au is designed as 200 GeV/(nucleon pair). The collider tunnel and target halls exist as does the liquid He refrigeration plant for the use of superconducting magnets in the collider configuration. Several prototype dipoles and one quadrupole have been built and tested and the project is ready for construction as soon as funding becomes available. The injection scheme for the collider consists of two tandem accelerators to provide the ion beams, and a synchrotron booster that can accelerate partially stripped ions to energies just below 1 GeV/nucleon where full stripping can be done at a reasonable efficiency. The beams will then be accelerated further in the BNL-AGS to  $\frac{Z}{A} \times 29$  GeV/c per nucleon and injected into RHIC. The tandems and the AGS are existing machines, that have delivered  $^{16}\text{O}$  and  $^{28}\text{Si}$  beams for physics experiments over the past two years at 14.5 GeV/c per nucleon. The synchrotron booster is under construction.

The scientific foundation for RHIC is of course intimately connected with the ideas of a possible phase transition from the confined hadronic state of quark matter, to a state where quarks (and gluons) can move freely over distances many (several) times the nucleonic diameter (quark-gluon plasma). An important part of the rationale for the choice of energy of RHIC, relies on the idea of transparency developing from full "stopping" with increasing bombarding energy. It is also important that energy densities of many times that of the ground state of cold nuclear matter can be reached in ion-ion collisions. In this talk, we will examine whether the two latter premises seem to hold true in view of the data from A+A collisions at the Brookhaven AGS-Tandem Complex and at the CERN-SPS. Finally, a few comments are made on measured slopes of hadronic  $p_{\perp}$  spectra.

### 2. Comments on nuclear "stopping" results

In their analysis of p+A data, Busza and Goldhaber<sup>1,2/</sup> found that an incoming proton at  $\approx 100$  GeV/c (in the lab frame) would lose  $\approx 2$  units of rapidity by traversing a Pb nucleus along

MASTER

a diameter. Under the assumption that this result does not depend on bombarding energy, one would conclude that nucleons with less than two units of rapidity to start with, would lose all of their rapidity in a central collision with a Pb nucleus. For a symmetric collision stopping should prevail for beam rapidities below 4 (2 in the c.m. system), i.e. for beams below  $\approx 60$  GeV/nucleon in the c.m. system.

There are presently two bodies of data relevant to these expectations. The first is from zero degree calorimeter measurements by CERN WA-80<sup>3/</sup> together with results from BNL-E802<sup>4/</sup>.

Figure 1 shows the E-802 results. The zero degree calorimeter is limited to an acceptance of  $\pm 0.3^\circ$  for these data. The two upper frames show results with a minimum bias trigger for a Au target (left) and an Al target (right). The beam was  $^{28}\text{Si}$  at 14.5 GeV/c per nucleon. Both distributions are broad, spanning from just below the beam kinetic energy at  $\approx 380$  GeV towards zero. For the Al target the distribution falls off at low energies, while for Au a peak is observed at  $\approx 20$  GeV. With a central trigger (high charged-particle multiplicity) the picture changes, in that the high energy part of the spectrum becomes suppressed. For Al the spectrum peaks at  $\approx 80$  GeV, showing that there are 5 to 6 spectators, while for Au the peak at  $\approx 20$  GeV dominates the spectrum. If the acceptance is increased to  $\pm 3^\circ$ , the above features do not change, although the 20 GeV Au peak becomes somewhat broader.

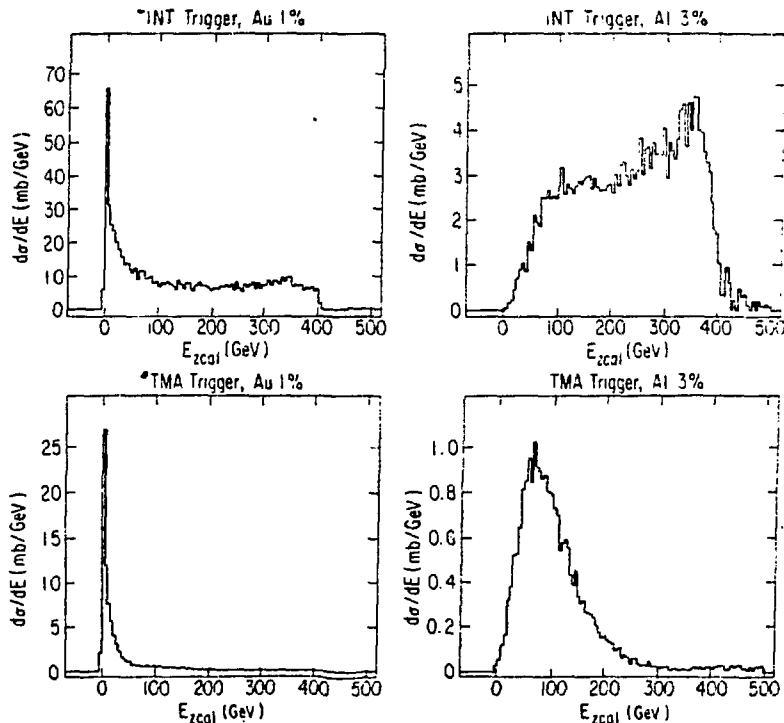


Fig. 1: Energy spectra from the E802 beam calorimeter

The interpretation of the above observations is straightforward. For Si+Al, collisions with total overlap of the two equally sized nuclei are rare and typical central collisions have only partial overlap. For Au, the projectile is much smaller than the target, and completely overlapping collisions happen often ( $\approx 10\%$  of all interactions). The fact that essentially no energy goes forward after a central Si+Au collision is indicative of "full" stopping.

In the WA-80  $^{16}\text{O}$  beam results<sup>3/</sup>, at 60 GeV/c per nucleon bombarding energy, the overall trend in going from light ( $^{12}\text{C}$ ) to heavy ( $^{197}\text{Au}$ ) targets is similar to the trends discussed above: on the light targets few events take place with  $\approx$ zero energy left in the beam while for Au the spectrum still peaks at  $\approx 40$  GeV, although the peak is less dominant than at the lower AGS energy. At 200 GeV/c per nucleon the peak in the  $^{16}\text{O} + ^{197}\text{Au}$  spectrum has moved up in energy to  $\approx 500$  GeV, and none of the lighter targets show a low energy peak.

We may conclude that "full" stopping is still possible at 60 GeV/nucleon for central collisions of  $^{16}\text{O} + \text{Au}$ , but at 200 GeV/nucleon there is always energy going forwards, i.e. "transparency" is setting in.

If the above interpretation of the zero-energy peak in the zero-degree calorimeter as being an indicator of "full" stopping is correct, it is implied from data of Ref. 3 that a Ag nucleus is not large enough to fully stop  $^{16}\text{O}$  at 60 GeV/nucleon beam energy.

The second body of data comes from lead-glass calorimeters, where the electromagnetic energy from  $\pi^0 \rightarrow 2\gamma$  and  $\eta^0 \rightarrow 2\gamma$  is measured. If the lead glass calorimeter has an acceptance that covers the maxima of the pseudo-rapidity distributions for the various targets, they give a measure of the energy of created  $\pi^0$  and  $\eta^0$  that is largely free of acceptance corrections for the slightly different kinematics of targets with different masses. The lead-glass arrays used in E802<sup>5,6/</sup> satisfy this acceptance condition. The results of Fig. 2 are from  $^{16}\text{O} + \text{A}$  at 14.5 GeV/c per nucleon and shows the total energy measured in an azimuthally symmetric lead-glass arrangement (for details see Ref. 5). One feature of interest is the high energy behavior of the  $E_{TOT}^0$  spectrum for Cu and for Au. If the Cu curve is multiplied by  $\times 5$ , it coincides with the Au curve, and both corresponds to 16 geometrically weighted convolutions of the p+Au spectrum over the beam nucleons (see Ref. 6 for details). Thus the  $\pi^0$  and  $\eta^0$  energy production from  $^{16}\text{O} + \text{Au}$  and  $^{16}\text{O} + \text{Cu}$  are the same for the highest energies observed, no more energy is produced with Au than with Cu. We may conclude that a nucleus of the size of Cu is enough to "fully" stop  $^{16}\text{O}$  at this bombarding energy, at least as regards energy flow from produced  $\pi^0$  and  $\eta^0$ . Preliminary E802 results for Si+A are in full accordance with the above discussion, the high energy edges for Cu, Ag, and Au are identical except for a cross section factor. The cross section factors may be interpreted geometrically, as the cross sections for complete overlap of projectile and target.<sup>5,6/</sup> An interpretation along these lines is not possible for the WA-80 calorimetry

data, because of acceptance effects (see e.g., Ref. 3).

It may be concluded that in regard to "stopping" the present data support the picture underlying the RHIC scenario, and demonstrates the onset of transparency for energies at  $\approx 200$  GeV/nucleon in fixed target mode.

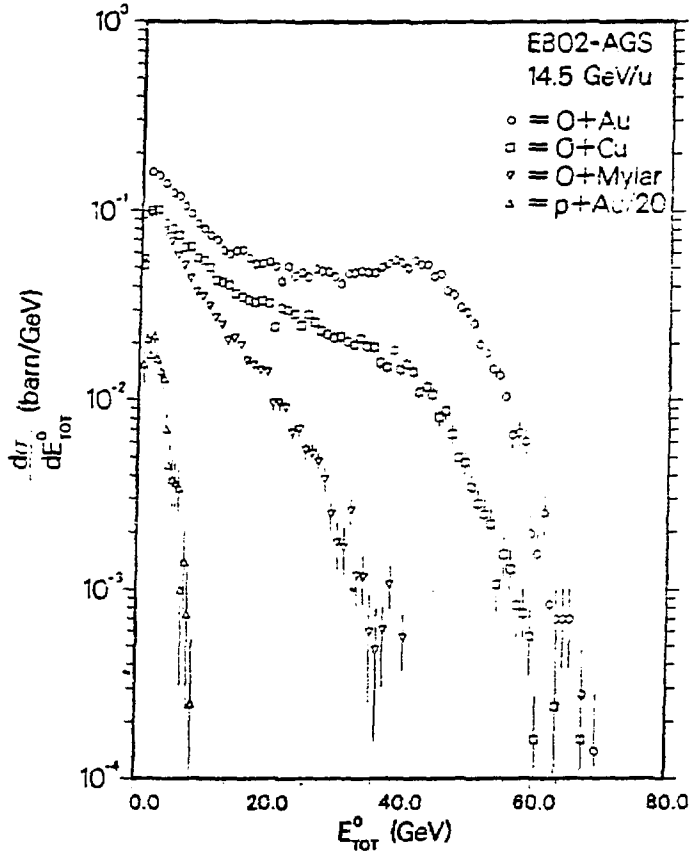


Fig. 2: Energy spectra from the E802 lead-glass array

### 3. Comments on energy densities

An energy density behaves under Lorentz transformation as the 44 component of the kinetic energy-momentum tensor<sup>7/</sup>, so if  $\epsilon$  is the density of a volume element in its local rest system, the density observed in the lab system is

$$\epsilon_{lab} = \epsilon \gamma^2 \quad (1)$$

when the local rest system travels with velocity  $\beta$  relative to the lab system, and  $\gamma = (1 - \beta^2)^{-1/2}$ . Hence a discussion of energy densities involves a discussion of reference system. In the extreme limit of full transparency, Bjorken<sup>8/</sup> has derived a formula, that connects the measured transverse energy density  $dE_{\perp}/dy$  in rapidity to the energy density in the hot, baryon free region between

the collision partners after the nuclear encounter

$$\epsilon = \frac{dE_{\perp}}{dy} (\pi R^2 \tau_0)^{-1} \quad (2)$$

$R$  is the radius of the smaller of the colliding nuclei and  $\tau_0$  is a typical time, usually taken as 1 fm. Equation (2) evidently does not apply in the AGS/CERN energy region, but has nonetheless been used as a reference. The obvious reason for using Eq. (2) is that no experiment has so far measured the relevant volume, from which the observed radiation originated. Applied directly, Eq. (2) gives values of  $\epsilon \approx 1$  GeV/fm<sup>3</sup> at the AGS energies<sup>/5,9/</sup> and  $\approx 2$  GeV/fm<sup>3</sup> at 200 GeV/nucleon (Refs. 3, 10, 11). At AGS energies use of a fireball-model to define the reference frame and the volume does not change<sup>/5,8/</sup> the estimated  $\epsilon$ , while a Landau shock front estimate (see e.g., Ref. 12) gives a larger value.

If the values quoted above are at all realistic, the indication is that densities of interest are being reached, from 6 to maybe over 10 times those of nuclear ground states. Thus, accepting the rather uncertain state of affairs, we may conclude that nothing argues strongly against the premise, that considerable densities may be reached in nucleus-nucleus collisions.

#### 4. Comments on slopes of $p_{\perp}$ -spectra

It is customary to present particle momentum spectra as  $E(d^3\sigma/dp^3)$  plotted versus  $p_{\perp}$ . Equivalent forms are often used,

$$E(d^3\sigma/dp^3) = d^3\sigma/(dp_x dp_y dy) = d^3\sigma/(p_{\perp} dp_{\perp} d\theta dy) \quad (3)$$

and sometimes the invariant cross section is integrated over the azimuthal angle ( $\theta$ ) and/or over rapidity ( $y$ ),

$$\int_0^{2\pi} E \frac{d^3\sigma}{dp^3} d\theta = 2\pi \frac{d^2\sigma}{p_{\perp} dp_{\perp} dy} \quad (4)$$

assuming that there is no explicit dependence on  $\theta$ .

Data of  $E(d^3\sigma/dp^3)$  plotted against  $p_{\perp}$  often look as an exponential and are parameterized as

$$E(d^3\sigma/dp^3) = \alpha(y) e^{-p_{\perp}/t(y)}. \quad (5)$$

Sometimes the data are integrated over rapidity  $y$  before parametrization, and the resulting slope then represents an averaging over the rapidity interval

$$\int_{y_1}^{y_2} dy E(d^3\sigma/dp^3) = \alpha' e^{-p_{\perp}/t}. \quad (6)$$

A tabulation of selected slope parameters from the CERN experiments are given below.

Table 1

Reaction	Particle	E/A (GeV)	Slope Parameter $t$		$y_2$	$y(\text{mid})$	Ref.
			$t$ (MeV/c)	$y_1$			
$^{16}\text{O}+\text{W}$	$(\pi^-)$	200	190	0.9	1.9	3.0	13
$^{16}\text{O}+\text{Au}$	$(\pi^-)$	200	153	2.0	3.0	3.0	14
$^{16}\text{O}+\text{Au}$	$\pi^0$	200	210	1.5	2.1	3.0	15
$^{16}\text{O}+\text{Au}$	$\pi^0$	60	200	1.5	2.1	2.0	15

$(\pi^-)$  stands for negatively charged particles, dominated by  $\pi^-$ . Errors on the slopes are typically less than  $\pm 10$  MeV/c and the  $p_\perp$  range (which differs from experiment to experiment) is from 0.5 GeV/c to  $\approx 2$  GeV/c. Preliminary data<sup>/16/</sup> from E802 at 14.5 GeV/c  $^{28}\text{Si}+\text{Au}$  show  $\pi^-$  slope parameters near 170 MeV/c for rapidities just below mid-rapidity and  $\approx 150$  MeV/c just forward of mid-rapidity. The data show a rapidity dependence towards smaller slope parameters with increasing rapidity. Within the spread of the numbers, it is fair to say that there is little variation in the  $\pi$  slope parameter at mid-rapidity in going from 14.5 GeV/nucleon  $^{28}\text{Si}$  to 200 GeV/nucleon  $^{16}\text{O}$ . p+A data from CERN exhibit very similar slopes; there are no p+A data from BNL.

Recalling that  $\pi$  slope parameters at the Bevalac (see e.g., Ref. 17) were much smaller ( $\leq 100$  MeV/c), it is clear that a "saturation" sets in with increasing bombarding energy.

One may ask: Is it possible to give a thermal interpretation of  $E(d^3\sigma/dp^3)$  versus  $p_\perp$  slopes? The experimental data at present are not sufficient to answer this question. We shall nonetheless offer a few remarks on the subject. Assume that the particles are emitted from a single thermal source with a Boltzman distribution in total energy  $E$ ,

$$P(p) = (4\pi m^2 T K_2(\frac{m}{T}))^{-1} e^{-E/T} \quad (7)$$

where  $P(p)$  is the probability of finding a particle of rest mass  $m$  with momentum between  $p$  and  $p + dp$ .  $T$  is the temperature of the source, and  $E^2 = p^2 + m^2$ .  $K_2$  is a function related to a Hankel function of second order of purely imaginary argument<sup>/18/</sup>.

Equation (7) can be recast into the variables  $p_\parallel$ ,  $p_\perp$ , and  $\theta$  and integrated over  $\theta$  and  $p_\parallel$ , (see also Eq. (3))

$$P(p_\perp)p_\perp dp_\perp = \int_{-\infty}^{\infty} dp_\parallel \int_0^{2\pi} d\theta P(p)p_\perp dp_\perp = (m^2 T K_2(\frac{m}{T}))^{-1} m_\perp K_1(\frac{m_\perp}{T}) p_\perp dp_\perp \quad (8)$$

where  $m_\perp = (m^2 + p_\perp^2)^{1/2}$  and  $K_1$  is a function related to a Hankel function of the first order (Ref. 18). Noting that  $p_\perp dp_\perp = m_\perp dm_\perp$ , Eq. (8) can be written

$$P(m_\perp) = (m^2 K_2(\frac{m}{T}))^{-1} \frac{m_\perp}{T} K_1(\frac{m_\perp}{T}) \quad (9)$$

i.e., for given mass and temperature the entire dependence on kinematical variables is in  $m_{\perp}$ . For large values of  $\frac{m_{\perp}}{T}$ , i.e. for

$$m_{\perp} \gg T \quad (10a)$$

$K_1$  becomes near exponential<sup>/18/</sup>, and

$$P(m_{\perp}) = (m^2 K_2(\frac{m}{T}))^{-1} (\frac{\pi}{2})^{1/2} (\frac{m_{\perp}}{T})^{1/2} e^{-\frac{m_{\perp}}{T}}. \quad (10)$$

Thus a plot of  $\frac{d\sigma}{dm_{\perp}}$  versus  $m_{\perp}$  gives a near exponential fall off with increasing  $m_{\perp}$  with a slope parameter that equals the temperature, when  $m_{\perp} \gg T$ .

Turning back to an interpretation of slope parameters from plots of Eqs. (5) or (6), we note that Eq. (8) gives a complicated behavior as function of  $p_{\perp}$ ,

$$N(p_{\perp}) dp_{\perp} \propto (m^2 + p_{\perp}^2)^{1/2} K_1 \left( \frac{(m^2 + p_{\perp}^2)^{1/2}}{T} \right) dp_{\perp} \quad (8a)$$

where  $N(p_{\perp})$  is the number of emitted particles with transverse momentum between  $p_{\perp}$  and  $p_{\perp} + dp_{\perp}$ . While Eq. (8a) is near exponential in  $m_{\perp}$  for  $m_{\perp} \gg T$ , it is not exponential in  $p_{\perp}$  until  $p_{\perp}$  satisfies

$$p_{\perp} \gg m. \quad (8b)$$

We thus have two conditions to satisfy for an exponential behavior of  $d^2\sigma/dp_{\perp}^2$ , namely Eqs. (8b) and (10a); the latter may be written (taking  $\gg$  to mean  $> 2\times$ ),

$$p_{\perp} > (4T^2 - m^2)^{1/2}. \quad (10b)$$

For pions the requirement is  $p_{\perp} > 400$  MeV/c for  $T \simeq 200$  MeV, which is fulfilled by the numbers quoted above. For kaons, Eq. (8b) is the sharper and requires  $p_{\perp} > 1$  GeV/c (using  $\gg$  to mean  $> 2\times$ ). Proton spectra plotted as invariant cross section versus  $p_{\perp}$  are not expected to be near exponential in  $p_{\perp}$  until  $p_{\perp} > 2$  GeV/c. The curvature of the  $K_1$  function for  $p_{\perp}$  values near  $m$ , may easily yield a totally erroneous temperature. The natural variable is not  $p_{\perp}$  but  $m_{\perp}$ .

Let us finally note, that the systematics of pion spectral slope parameters may possibly reflect a statement about a temperature saturation. The fact that p+A spectra exhibit a very similar trend certainly means that the phenomena is not exclusive for A+A collisions. It will be very exciting to see spectra from very heavy beams and at much higher energies. Is there really a universal maximum slope value of  $\simeq 200$  MeV/c for pion spectra? We need RHIC badly!

### Acknowledgements

This research was supported by the U. S. Department of Energy, Division of Basic Energy Sciences under Contract No. DE-AC02-76CH00016.

## References

1. W. Busza, Nucl. Phys. A418 (1984) 635c.
2. W. Busza and A. Goldhaber, Phys. Lett. 139B (1984) 235.
3. S. P. Sorensen et al., The WA-80 Collaboration, Z. Phys. C 38 (1988) 3.
4. E. Duek et al., The E-802 Collaboration, Contribution to the *Third Int. Conf. on Nucleus-Nucleus Collisions*, Saint Malo, France, 1988.
5. T. Abbott et al., The E-802 Collaboration, Phys. Lett. B197 (1987) 285.
6. L. P. Remsberg et al., The E-802 Collaboration, Z. Phys. C 38 (1988) 35.
7. *The Theory of Relativity*, C. Moller, University Press, Oxford, 1955.
8. D. Bjorken, Phys. Rev. D27 (1983) 140.
9. P. Braun-Munzinger et al. Z. Phys. C 38 (1988) 45.
10. F. Corriveau et al., The Helios Collaboration, Z. Phys. C 38 (1988) 15.
11. W. Heck et al., The NA-35 Collaboration, Z. Phys. C 38 (1988) 19.
12. M. Gyulassy, Z. Phys. C 38 (1988) 361.
13. H. W. Bortels, The NA-34 Collaboration. Z. Phys. C 38 (1988) 85.
14. H. Stroebele, The NA-35 Collaboration, Z. Phys. C 38 (1988) 89.
15. H. Loehner, The WA-80 Collaboration, Z. Phys. C 38 (1988) 97.
16. G. Stephans, The E-802 Collaboration, Contribution to the *Third Int. Conf. on Nucleus-Nucleus Collisions*, Saint-Malo, France, 1988.
17. S. Nagamiya, Nucl. Phys. A418 (1984) 239c.
18. M. Abramowitz and I. A. Stegun, *Handbook of Mathematical Functions*, Dover Publications, Inc., New York, 1972.

## DISCLAIMER

This report was prepared as an account of work sponsored by an agency of the United States Government. Neither the United States Government nor any agency thereof, nor any of their employees, makes any warranty, express or implied, or assumes any legal liability or responsibility for the accuracy, completeness, or usefulness of any information, apparatus, product, or process disclosed, or represents that its use would not infringe privately owned rights. Reference herein to any specific commercial product, process, or service by trade name, trademark, manufacturer, or otherwise does not necessarily constitute or imply its endorsement, recommendation, or favoring by the United States Government or any agency thereof. The views and opinions of authors expressed herein do not necessarily state or reflect those of the United States Government or any agency thereof.